

Joint Spatial- and Doppler-based Ego-Motion Estimation for Automotive Radars

Michael Barjenbruch¹, Dominik Kellner¹, Jens Klappstein², Juergen Dickmann² and Klaus Dietmayer¹

Abstract—An ego-motion estimation method based on the spatial and Doppler information obtained by an automotive radar is proposed. The estimation of the motion state vector is performed in a density-based framework. Compared to standard vehicle odometry the approach is capable to estimate the full two dimensional motion state with three degrees of freedom. The measurement of a Doppler radar sensor is represented as a mixture of Gaussians. This mixture is matched with the mixture of a previous measurement by applying the appropriate ego-motion transformation. The parameters of the transformation are found by the optimization of a suitable join metric. Due to the Doppler information the method is very robust against disturbances by moving objects and clutter. It provides excellent results for highly nonlinear movements. Real world results of the proposed method are presented. The measurements are obtained by a 77 GHz radar sensor mounted on a test vehicle. A comparison using a high-precision inertial measurement unit with differential GPS support is made. The results show a high accuracy in velocity and yaw-rate estimation.

I. INTRODUCTION

Advanced driver assistant systems (ADAS) highly improve the safety of modern vehicles. Therefore ADAS rely on different sensor systems, like cameras, laser scanners and radar sensors. To create a reliable representation of the static and dynamic environment of the ego-vehicle these sensors use mapping and tracking algorithms, respectively. Beside the measurements these algorithms also require exact information about the motion state of the vehicle they are mounted on. For mapping applications a precise ego-motion is essential to integrate new measurements into the map. For tracking systems the ego-motion has to be compensated to obtain the absolute motion of the tracked object.

Today's electronic stability control systems obtain this information by wheel speed measurements and inertial sensors, such as gyroscopes and accelerometers. While this methods provides a good short-term accuracy on high friction surfaces, they suffer from drift over time and slippery or uneven road surfaces. If these errors occur, new measurements are misaligned with respect to a reference coordinate system. For mapping algorithms it would cause blurring and thus an inaccurate localization. For tracking algorithms the impact is even more severe. An ego-motion error pulls tracks the wrong directions and induces bogus velocities. To overcome these flaws alternative methods to obtain the ego-vehicle's motion state are desired.

¹Michael Barjenbruch, Dominik Kellner and Klaus Dietmayer are with Institute of Measurement, Control and Microtechnology, Ulm University, Germany, Email: firstname.lastname@uni-ulm.de

²Jens Klappstein and Juergen Dickmann are with Daimler AG, Ulm, Germany, Email: firstname.lastname@daimler.com

An alternative approach to obtain the ego-vehicle's motion is based on environment sensing. The ego-motion is deduced from the relative velocity or relative change in position of the static surrounding of the ego-vehicle relative to the ego-vehicle itself. Positions are easy to measure, but a certain integration time is necessary to derive the motion, which leads to inaccuracy in fast motion changes. Velocity information provides a better basis for deriving the motion state, however velocity information is harder to obtain and can only be measured indirectly, e.g. the radial Doppler-velocity obtained by radar sensors. In this paper a novel estimation method is presented, which is able to estimate the full two dimensional (2D) motion state of the ego-vehicle with very high accuracy using only a single radar sensor.

The reminder of this paper is structured as follows: in Section II existing ego-motion estimation approaches are review. A novel radar-based ego-motion estimation algorithm is introduced in Section III. Section IV contains experimental results obtained by real world measurements. Finally, in Section V the proposed estimation method is reviewed and evaluated.

II. RELATED WORK

Several techniques using different sensor systems have been proposed retrieving ego-vehicles motion. In this section approaches using different technologies are reviewed.

A. Wheel-based odometry and inertial sensors

Wheel-based odometry provides ego-motion information fast and with a high availability. These estimates are biased by errors like wrong wheel diameters and suffer from bad traction, especially from slipping. Inertial navigation systems (INS) and global navigation satellite systems (GNSS) can be used to tackle the problem [1]. However, the availability of GNSS is limited and low-cost INS have a poor long-term stability and suffer from systematic errors [2].

B. Visual odometry

Visual odometry techniques either employ monocular or stereoscopic cameras [3]. The advantage of visual odometry compared to wheel-based techniques is the direct estimation of the speed over ground. Thus the friction between wheels and ground has no influence. To obtain the monocular visual odometry features are tracked across several camera images. Then 3D points are reconstructed. Using a stereoscopic camera rig the 3D information is available immediately [4]. Finally, the 3D points are used to compute the pose change between two consecutive images. This change corresponds

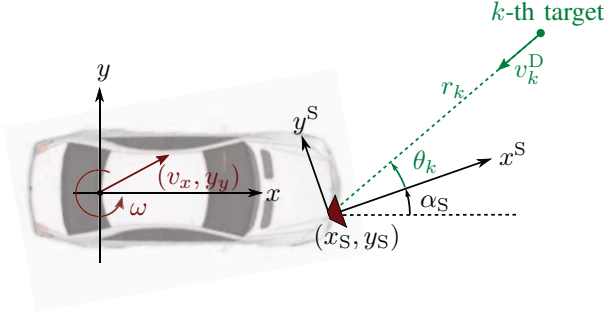


Fig. 1. Vehicle and sensors coordinate system. The vehicle's motion parameters are v_x , v_y and ω . θ_k , r_k and v_k^D are the parameters of the k -th target measured by the radar sensor. The vehicle coordinate system is given by x and y and the sensor coordinate system by x^S and y^S .

to the ego-motion of the vehicle. However, visual odometry only works if visual features can be extracted reliably, which can be difficult in bad weather conditions.

C. Laser scanner

In [5] a laser scanner (LIDAR) is used for ego-motion estimation by scan matching. This is achieved similarly to the visual odometry approach in two steps. In the first step the movement between two consecutive scans is obtained by matching them using the iterative closest point (ICP) algorithm. The solution is used as a starting value to integrate the current scan into a grid map of older scans. The exact solution is found by random sampling.

D. Radar sensor

The first methods proposed to determine the ego-motion by radar apply sensors mounted underneath the vehicle pointing forwards to the road surface [6]. However, these methods highly depend on the quality of the road surface and the radar sensor cannot be used for any other purpose. [7] analyzes the relation between the azimuth angle and the radial Doppler velocity to obtain the ego-vehicle's motion state. Compared to position-based approaches this method provide excellent results for highly nonlinear movements. However, it requires two radar sensors mounted in different locations. The method presented in this paper is capable to estimate the full 2D motion state with just a single Doppler-radar and provides competitive results.

III. ESTIMATION METHOD

The proposed algorithm performs a density-based estimation of the ego-vehicle's motion state. The estimation is achieved by matching the current with the previous measurement. The targets' positions are registered with respect to their particular uncertainty. From the displacement between two measurements the motion state is estimated. Further the measured Doppler velocity is compared with the expected velocity according to the motion state. Both metrics are combined into a joint optimization problem. The overall algorithm is outlined in Fig. 2.

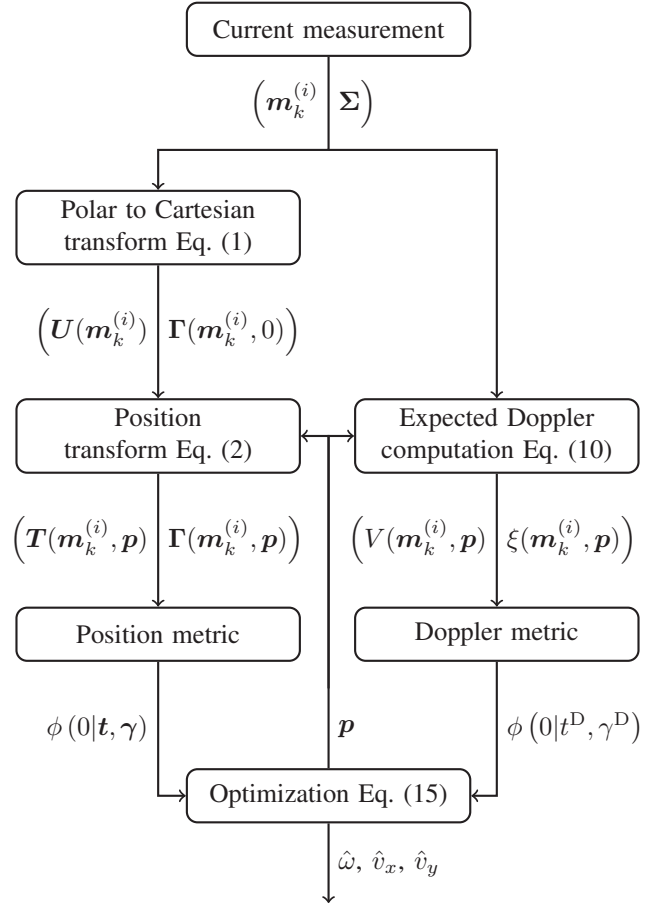


Fig. 2. Flow chart of the position-based motion estimation. The operations applied to each detected target, are depicted. The resulting values of each step with the corresponding covariances are shown.

A. Measurement model

In each measurement the radar sensor detects K targets. Each target is detected by its radar cross-section. The vector m_k of the k -th target comprises its properties: $m_k = [\theta_k, r_k, v_k^D]^T$, where θ_k denote the angle between the front of the sensor and the target, r_k the distance between the sensor and the target and v_k^D the Doppler velocity of the target, respectively. The Doppler velocity is the radial projection of the relative velocity between the target and sensor. For each value the error is assumed to be normal distributed with the variances of σ_θ^2 , σ_r^2 and σ_v^2 , respectively. Thus the covariance matrix Σ for each target is a diagonal matrix with the three variances on its main diagonal.

The origin of the vehicle coordinate system is at the center of the vehicles rear axle as shown in Fig. 1. The y-axis is aligned with the rear axle. The sensor coordinate system is located at the position (x_S, y_S) in the vehicle coordinate system and rotated by the angle α_S . Thus this angle corresponds with the sensor's mounting angle.

The motion state of the ego-vehicle $p = [\omega, v_x, v_y]^T$ is described by its velocity in x- and y-direction v_x, v_y and its yaw-rate ω . These three parameters (3 DOF) specify the movement of a rigid object in a plane completely.

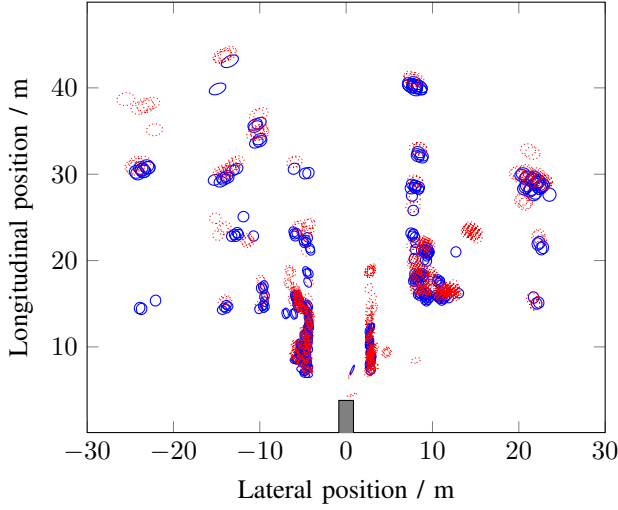


Fig. 3. An example depicting the three sigma uncertainty of a position measurement in solid blue. The ego-vehicle's position is marked with a gray box. The uncertainty of the previous measurement is shown in dotted red. The distance between the two measurements correspond to the movement between them.

B. Spatial-based metric

Prior to the matching, the targets have to be transformed into a common coordinate system. Therefore two transformations are necessary. A transformation from the polar measurement space into the Cartesian space simplifies the incorporation of the motion information. Then, the displacement caused by the motion is compensated to compare the current measurement with the previous measurement. The comparison is done by representing the measurements with mixtures of Gaussians, which are matched by a metric.

First, each target has to be transformed from polar into Cartesian coordinates using the transformation

$$\mathbf{U}(\mathbf{m}_k) = \begin{bmatrix} r_k \cos(\theta_k + \alpha) + x_S \\ r_k \sin(\theta_k + \alpha) + y_S \end{bmatrix}. \quad (1)$$

Second, targets from the current measurement have to be transformed into the reference system of a previous measurement according to the current motion state p . This is done by the transformation:

$$\mathbf{T}(\mathbf{m}_k, p) = \begin{bmatrix} \cos(\omega\tau) & -\sin(\omega\tau) \\ \sin(\omega\tau) & \cos(\omega\tau) \end{bmatrix} \mathbf{U}(\mathbf{m}_k) + \begin{bmatrix} v_x\tau \\ v_y\tau \end{bmatrix}, \quad (2)$$

where τ denotes the time between the two measurements.

The covariance matrices of the transformed targets are approximated by $\mathbf{\Gamma}(\mathbf{m}_k, p) = \mathbf{J}(\mathbf{m}_k, p) \mathbf{\Sigma} \mathbf{J}^T(\mathbf{m}_k, p)$, using the Jacobian matrix according to [8]

$$\mathbf{J}(\mathbf{m}_k, p) = \begin{bmatrix} \frac{\partial \mathbf{T}(\mathbf{m}_k, p)}{\partial \theta_k} & \frac{\partial \mathbf{T}(\mathbf{m}_k, p)}{\partial r_k} & \frac{\partial \mathbf{T}(\mathbf{m}_k, p)}{\partial v_k^D} \end{bmatrix}. \quad (3)$$

In this case the last column is zero as the position is independent from the Doppler velocity. An example of the resulting covariances is shown in Fig. 3.

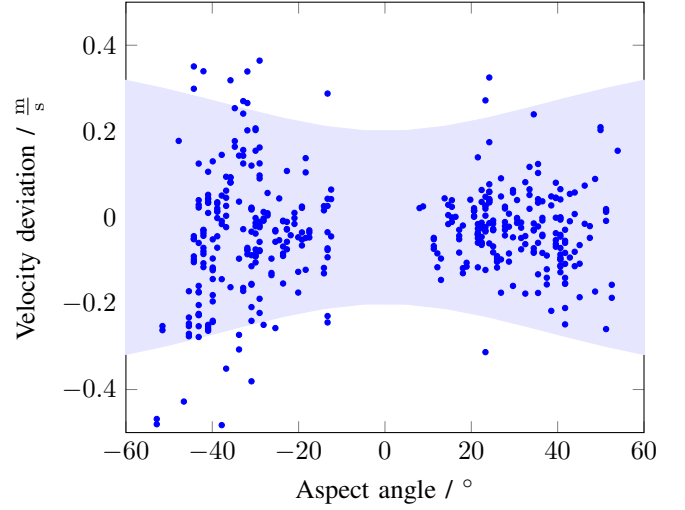


Fig. 4. An example showing the discrepancy between the measured Doppler velocity and the expected velocity for stationary targets with the three sigma corridor. Moving targets and clutter appear outside this corridor. Due to the dependence of covariance on the angle, the corridor is widened for larger aspect angles.

With transformations for both measurements to the Cartesian space a matching is possible. They are matched by applying a robust point set registration algorithm [9]. Therefore the measurements are considered as a mixture of Gaussians, where each target is represented by a Gaussian distribution. With the Gaussian density function $\phi(\mathbf{x}|\mathbf{m}, \mathbf{\Sigma})$ for δ DOF

$$\phi(\mathbf{x}|\mathbf{m}, \mathbf{\Sigma}) = \frac{\exp\left[-\frac{1}{2}(\mathbf{x} - \mathbf{m})^T \mathbf{\Sigma}^{-1}(\mathbf{x} - \mathbf{m})\right]}{\sqrt{(2\pi)^\delta |\mathbf{\Sigma}|}}, \quad (4)$$

the probability density function $f(\mathbf{x})$ of a measurement in polar space is given by

$$f(\mathbf{x}) = \frac{1}{K} \sum_{k=1}^K \phi(\mathbf{x}|\mathbf{m}_k, \mathbf{\Sigma}). \quad (5)$$

Due to the radar sensor's measurement technique a constant covariance matrix is assumed in polar space and all targets are weighted equally. With the transformation (2) the density function (5) can be rewritten in terms of transformed Cartesian space as

$$f(\mathbf{x}) = \frac{1}{K} \sum_{k=1}^K \phi(\mathbf{x}|\mathbf{T}(\mathbf{m}_k, p), \mathbf{\Gamma}(\mathbf{m}_k, p)). \quad (6)$$

Two measurements are matched by the l_2 metric of two Gaussians $\phi(\mathbf{x}|\mathbf{m}, \mathbf{\Sigma})$ and $\phi(\mathbf{x}|\mathbf{m}', \mathbf{\Sigma}')$, which is given by $\phi(0|\mathbf{m} - \mathbf{m}', \mathbf{\Sigma} + \mathbf{\Sigma}')$, according to [10]. If the difference between the mean values $\mathbf{m} - \mathbf{m}'$ is minimized, the function provides the maximum value with respect to the joint covariance $\mathbf{\Sigma} + \mathbf{\Sigma}'$.

Thus the transformation between two measurements is evaluated by the metric function $d(p)$, given by

$$d(p) = \frac{1}{KN} \sum_{k=1}^K \sum_{n=1}^N \phi(0|\mathbf{t}, \gamma) \quad (7)$$

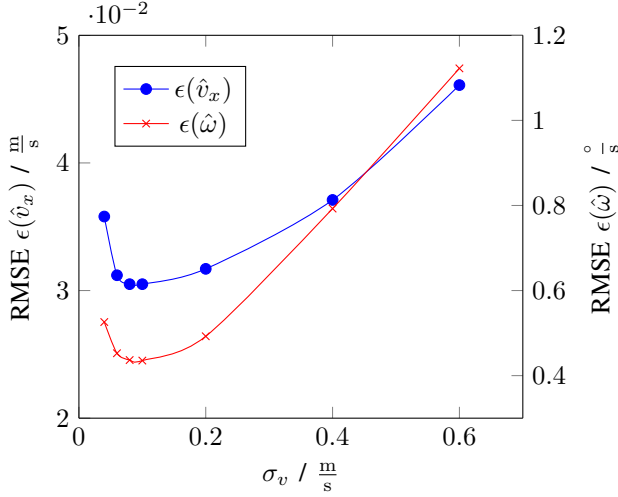


Fig. 5. The Doppler velocity standard deviation σ_v is varied while the distance and angular standard deviation σ_r and σ_θ are kept fixed. The impact on the RMSE of the estimated velocity \hat{v}_x and yaw-rate $\hat{\omega}$ is visible.

with the distance between the mean values \mathbf{t} and the summation of covariances γ

$$\mathbf{t} = \mathbf{T}(\mathbf{m}_k^{(i)}, \mathbf{p}) - \mathbf{T}(\mathbf{m}_n^{(i-1)}, 0), \quad (8)$$

$$\gamma = \Gamma(\mathbf{m}_k^{(i)}, \mathbf{p}) + \Gamma(\mathbf{m}_n^{(i-1)}, 0), \quad (9)$$

where i denote the current measurement containing K targets and $i - 1$ the previous one containing N targets. The transformation applied to the $(i - 1)$ -th measurement with zero motion $\mathbf{T}(\cdot, 0)$ equals the polar to Cartesian transformation $\mathbf{U}(\cdot)$. Therefore, only the spatial components of \mathbf{m}_k are part of the metric.

C. Doppler-based metric

Additionally to the position information the Doppler radar provides very precise velocity information. By matching the expected with the measured Doppler velocity the accuracy can be improved significantly. Further this step will suppress distortion by non-stationary objects in the vehicles environment. If the Doppler velocity of a target does not meet the expected velocity it will receive a very low weight in the metric function.

The expected Doppler velocity $V(\mathbf{m}_k, \mathbf{p})$ for a stationary target \mathbf{m}_k with the ego-vehicle being in a certain motion state \mathbf{p} can be computed as

$$V(\mathbf{m}_k, \mathbf{p}) = -(v_x - \omega y_S) \cos(\theta_k + \alpha_S) - (v_y + \omega x_S) \sin(\theta_k + \alpha_S). \quad (10)$$

The velocity of the sensor in the x-direction equals $v_x - \omega y_S$ and in the y-direction equals $v_y + \omega x_S$. If the radar sensor is moved, from its point of view, all stationary targets have the opposite relative velocity to the sensor. By computing the projection at angle $\theta_k + \alpha_S$ the Doppler velocity of a static target is obtained. The corresponding variance $\xi(\mathbf{m}_k, \mathbf{p})$ is approximated by the first derivative of the nonlinear

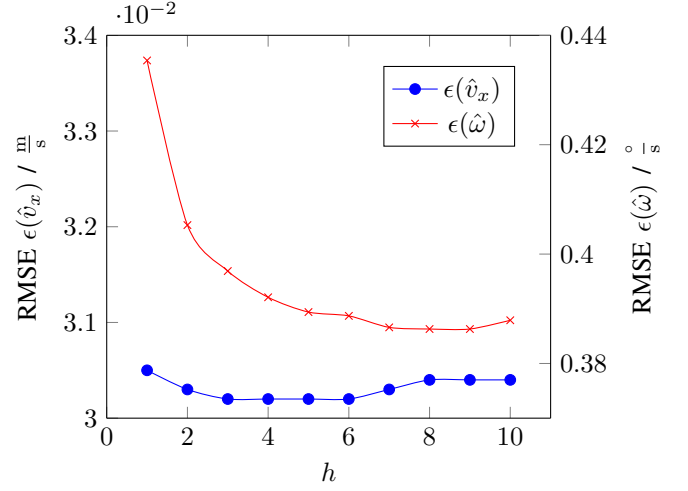


Fig. 6. The influence of the history length h is shown. Using multiple older measurements can help to reduce the RMSE of the estimated yaw-rate $\hat{\omega}$, while leaving the RMSE of the estimated velocity \hat{v}_x almost unaffected.

transform as in Eq. (3):

$$\xi(\mathbf{m}_k, \mathbf{p}) = \left(\frac{\partial V(\mathbf{m}_k, \mathbf{p})}{\partial \theta_k} \right)^2 \sigma_\theta^2. \quad (11)$$

With the measured and the expected Doppler velocity the Doppler weight $\phi(0|t^D, \gamma^D)$ is computed with

$$t^D = v_k^D - V(\mathbf{m}_k, \mathbf{p}), \quad (12)$$

$$\gamma^D = \sigma_v^2 + \xi(\mathbf{m}_k, \mathbf{p}). \quad (13)$$

t^D is the deviation between the measured expected velocity and γ^D is the sum of the variances. In Fig. 4 the ordinate of the points correspond t^D and the corridor is defined by γ^D .

D. Joint spatial- and Doppler-based ego-motion estimation

To perform a joint position and Doppler-based ego-motion estimation the Doppler weight $\phi(0|t^D, \gamma^D)$ is integrated into the position-based metric function Eq. (7) giving the joint position and Doppler-based metric

$$d^D(\mathbf{p}) = \frac{1}{KN} \sum_{k=1}^K \sum_{n=1}^N \phi(0|\mathbf{t}, \gamma) \phi(0|t^D, \gamma^D). \quad (14)$$

In order to estimate the motion state of the ego-vehicle the metric function $d^D(\mathbf{p})$ of Eq. (14) has to be maximized, leading to the optimization problem

$$\{\hat{\omega}, \hat{v}_x, \hat{v}_y\} = \underset{\omega, v_x, v_y}{\operatorname{argmax}} d^D(\mathbf{p}), \quad (15)$$

which can be solved by gradient-based or simplex optimization methods.

If no side-slip at the rear axle is assumed $v_y = 0$, the optimization problem can be reduced by one degree of freedom to

$$\{\hat{\omega}, \hat{v}_x\} = \underset{\omega, v_x}{\operatorname{argmax}} d^D(\mathbf{p})|_{v_y=0} \quad (16)$$

for more accurate results in the remaining two dimensions.

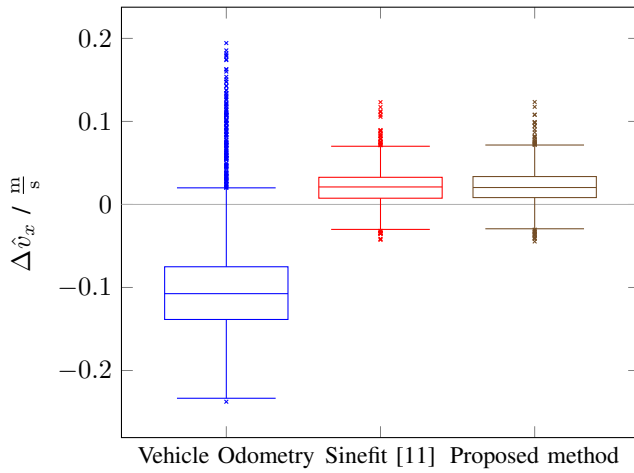


Fig. 7. The accuracy of the estimated velocity for different methods is compared.

Although the proposed estimation method requires just a single sensor to operate, it is straight forward to extend it to multiple sensors. The measurements of all sensors can be analyzed jointly, if the correct mounting parameters x_S , y_S and α_S are known for each sensor.

An improvement to the accuracy of the position matching is possible by using more than one previous measurement. Therefore the targets of the last h measurements are included as reference. Thereby the current measurement is compared with more than one older measurement. This is achieved very efficiently by transforming the $(i-1) \dots (i-h)$ measurements according to the (i) -th motion state after the estimation. When the $(i+1)$ -th measurement arrives, all previous measurement have the same reference position and alignment.

IV. EXPERIMENTAL RESULTS

The proposed method is evaluated with real world measurements. An automotive 77 GHz radar sensor with a bandwidth of 500 MHz and an update-rate of 15 Hz is used. The sensor is mounted at the front of the ego-vehicle. The vehicle is driven with an average speed of 30 km/h in an urban scenario. For the evaluation 1500 measurements are recorded. If not stated otherwise, a standard deviation of $\sigma_\theta = 0.5^\circ$ in azimuth, $\sigma_r = 0.2$ m in distance and $\sigma_v = 0.1 \frac{m}{s}$ in Doppler velocity are assumed. $\Delta\hat{x}$ denotes the difference between an estimated value \hat{x} and the true value x . The root mean squared error (RMSE) of an estimated parameter \hat{x} is denoted by $\epsilon(\hat{x})$. For reference the vehicle is equipped with a high-precision IMU with differential GPS support. The accuracy of the IMU is less than 2 cm.

In Fig. 5 the impact of the correctness of the assumed standard deviation in Doppler velocity is shown. This is achieved by varying the Doppler velocity standard deviation σ_v while the distance and angular standard deviation σ_r and σ_θ are kept fixed. The best results are achieved for a standard deviation of $\sigma_v = 0.1 \frac{m}{s}$. If the deviation is set lower, the Gaussians of the expected and measured Doppler

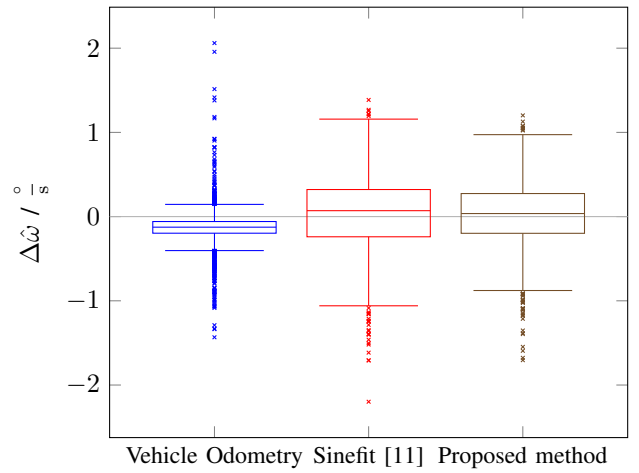


Fig. 8. Comparison of the estimation error of the yaw-rate for different estimation methods.

velocity do not overlap. If the deviation is set higher, the Doppler velocity has lower influence on the metric and so the matching is less efficient.

The history length h is analyzed in Fig. 6. The RMSE of the estimated velocity \hat{v}_x is almost constant at $0.03 \frac{m}{s}$. However, the RMSE of the estimated yaw-rate $\hat{\omega}$ depends on h . The RMSE is improved from $0.435 \frac{^\circ}{s}$ at $h = 1$ by 11% to $0.386 \frac{^\circ}{s}$ at $h = 8$.

In order to analyze the performance of the method in the 2 DOF case, the results of the proposed method are compared with the vehicle odometry from the FlexRay bus of the vehicle and another radar based method. The other method performs a regression by aligning a sine to the stationary targets in the θ - v^D -space [11]. From the parameters of the sine (amplitude and phase offset) \hat{v}_x and $\hat{\omega}$ are derived and therefore it is termed *Sinefit* in this paper.

The estimation accuracies for the velocity \hat{v}_x of the three methods are shown in Fig. 7. For the vehicle odometry the standard deviation is $0.072 \frac{m}{s}$ and the bias is $-0.095 \frac{m}{s}$. A standard deviation of $0.022 \frac{m}{s}$ and a bias of $0.021 \frac{m}{s}$ are achieved by the proposed method. The Sinefit method has exact the same standard deviation and mean for the velocity estimation. Thus the radar based methods are more than three times better than the vehicle odometry.

In Fig. 8 the estimation precision for the yaw-rate $\hat{\omega}$ is investigated. A standard deviation of $0.248 \frac{^\circ}{s}$ and a bias of $-0.136 \frac{^\circ}{s}$ is accomplished by the vehicle odometry. The Sinefit has a standard deviation of $0.447 \frac{^\circ}{s}$ and a bias of $0.034 \frac{^\circ}{s}$. The proposed method achieves a standard deviation of $0.386 \frac{^\circ}{s}$ and a bias of $0.016 \frac{^\circ}{s}$. Thus the vehicle odometry has a lower standard deviation than the radar based methods. However, the radar based methods provide a much better bias, which is important especially for dead reckoning. Comparing the radar based methods, the proposed method outperforms the Sinefit method in standard deviation and bias. Compared to the other methods, the proposed method has the least severe outliers.

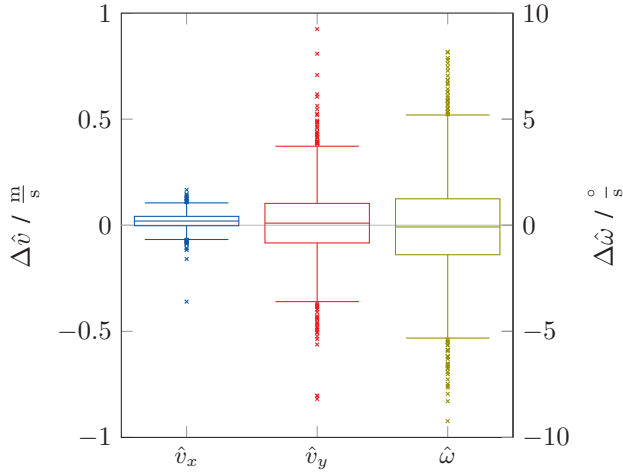


Fig. 9. Comparison of the precision of the estimated motion state parameters for the 3 DOF case.

The 3 DOF case is shown in Fig. 9. For the estimated longitudinal velocity \hat{v}_x the standard deviation is $0.037 \frac{\text{m}}{\text{s}}$ and bias is $0.020 \frac{\text{m}}{\text{s}}$. The estimation of the lateral velocity \hat{v}_y has a standard deviation of $0.178 \frac{\text{m}}{\text{s}}$ and a bias of $0.011 \frac{\text{m}}{\text{s}}$. A standard deviation of $2.607 \frac{\text{deg}}{\text{s}}$ and a bias of $-0.118 \frac{\text{deg}}{\text{s}}$ are achieved for the estimated yaw-rate $\hat{\omega}$. For the longitudinal velocity the 3 DOF case has comparable results to the 2 DOF case. Due to the additional degree of freedom the accuracy of the yaw-rate estimation is reduced compared to the 2 DOF case. Thus the 3 DOF model is only reasonable if significant lateral velocities are expected.

Figure 10 shows the position obtained by dead reckoning based on the motion state estimated with the proposed method. After a distance of 827 m the position error based on the vehicle odometry is 34.5 m. With the Sinefit a position error of 13.7 m is achieved. Whereas the proposed method has a position error of only 3.0 m. Thus the relative error is just 0.37% in relation to the length of the driven path.

V. CONCLUSIONS

A novel density-based method for ego-motion estimation with a Doppler radar is presented. Based on a mixture of Gaussians representation for the measurements two or more consecutive measurements are matched. The motion state of the ego-vehicle is derived by the transformations for matching these measurements. The method is applicable to estimate the full 2D motion state with 3 DOF with just a single Doppler radar sensor. In the 2 DOF case the method shows superior results in velocity estimation compared to the vehicle odometry. The yaw-rate estimation is better than the estimation reference radar method. Compared to the vehicle odometry the bias of the estimated yaw-rate is significantly lower. Especially if applied to dead reckoning the advantage of the proposed method is visible.

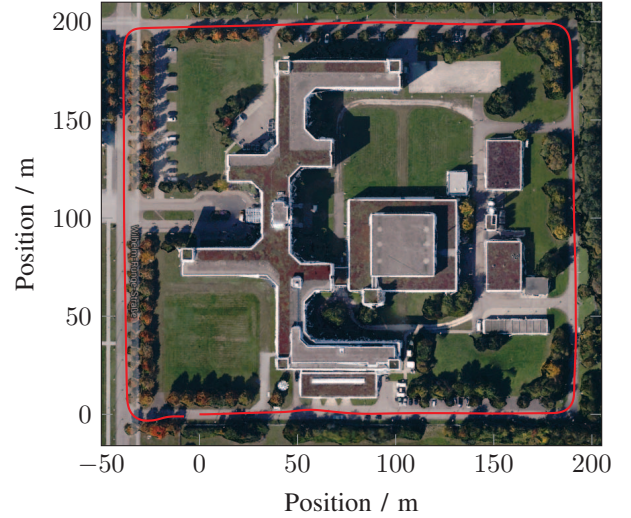


Fig. 10. Position according to dead reckoning based on the motion state estimated with the proposed method (aerial photo © 2015 Google)

REFERENCES

- [1] D.M. Bevlly, J. Ryu, and J.C. Gerdes, "Integrating INS Sensors With GPS Measurements for Continuous Estimation of Vehicle Sideslip, Roll, and Tire Cornering Stiffness," *IEEE Transactions on Intelligent Transportation Systems*, vol. 7, no. 4, pp. 483–493, Dec 2006.
- [2] J. Borenstein and L. Feng, "Measurement and correction of systematic odometry errors in mobile robots," *IEEE Transactions on Robotics and Automation*, vol. 12, no. 6, pp. 869–880, Dec 1996.
- [3] D. Nister, O. Naroditsky, and J. Bergen, "Visual odometry," in *Proceedings of the IEEE Computer Society Conference on Computer Vision and Pattern Recognition (CVPR)*, June 2004, vol. 1, pp. 1–652–I–659 Vol.1.
- [4] Hernán Badino, "A robust approach for ego-motion estimation using a mobile stereo platform," in *Complex Motion*, pp. 198–208. Springer, 2007.
- [5] T. Miyasaka, Y. Ohama, and Y. Ninomiya, "Ego-motion estimation and moving object tracking using multi-layer LIDAR," in *IEEE Intelligent Vehicles Symposium*, June 2009, pp. 151–156.
- [6] A. Hantsch and W. Menzel, "A 76GHz Folded Reflector Antenna for True Ground Speed Measurement," in *Proceedings of the German Microwave Conference*, 2006.
- [7] D. Kellner, M. Barjenbruch, J. Klappstein, J. Dickmann, and K. Dietmayer, "Instantaneous ego-motion estimation using multiple Doppler radars," in *IEEE International Conference on Robotics and Automation (ICRA)*, May 2014, pp. 1592–1597.
- [8] C.D. Ghilani, *Adjustment computations: spatial data analysis*, John Wiley & Sons, 2010.
- [9] B. Jian and B.C. Vemuri, "A robust algorithm for point set registration using mixture of Gaussians," in *Tenth IEEE International Conference on Computer Vision (ICCV)*, Oct 2005, vol. 2, pp. 1246–1251 Vol. 2.
- [10] D.W. Scott, "Parametric statistical modeling by minimum integrated square error," *Technometrics*, vol. 43, no. 3, pp. 274–285, 2001.
- [11] D. Kellner, M. Barjenbruch, J. Klappstein, J. Dickmann, and K. Dietmayer, "Instantaneous ego-motion estimation using Doppler radar," in *16th International IEEE Conference on Intelligent Transportation Systems (ITSC)*, Oct 2013, pp. 869–874.